



Implications of two backward blood spatter models based on fluid dynamics for bloodstain pattern analysis

P.M. Comiskey^a, A.L. Yarin^{a,*}, D. Attinger^b

^a Department of Mechanical and Industrial Engineering, University of Illinois at Chicago, 842 W. Taylor St., Chicago, IL 60607-7022, USA

^b Department of Mechanical Engineering, Iowa State University, 2529 Union Dr., Ames, IA 50011-1210, USA

ARTICLE INFO

Article history:

Received 14 September 2018

Received in revised form 11 May 2019

Accepted 13 May 2019

Available online 19 May 2019

Keywords:

Bloodstain pattern analysis

Gunshot blood spatter

Theoretical model

ABSTRACT

Bloodstain pattern analysis (BPA) is an integral part of crime scene investigation. For violent crimes involving gunshots, standard practice in police departments worldwide have some physical limitations. For instance, the effect of gravity and air drag on trajectories of blood droplets are neglected using current reconstruction methods, which results in a well-known overestimation of the height of the source of blood. As a consequence, more sophisticated models for blood spatter trajectory reconstruction are being developed, two of which are highlighted in the present work. They allow the prediction of bloodstain patterns produced from backward spattered blood droplets from blunt and sharp bullets. Our recent models attribute the splashing of blood to the Rayleigh–Taylor instability which arises when blood is accelerated towards lighter air. This physically-based description comes with the powerful predictive capability to correlate features of bloodstain patterns with the specific bullet and gun that produced them, as well as with the body position. The results of the numerical models were compared with four experiments simulating blood spatter deposition on a vertical wall through the number of stains produced, average stain area, and average impact angle at the surface, and the agreement found is fairly good. Moreover, further insight is obtained by probing and explaining the influence of observable parameters on the resulting spatter pattern, with the goal of aiding BPA experts evaluating a crime scene.

© 2019 Elsevier B.V. All rights reserved.

1. Introduction

Bloodstain pattern analysis (BPA) is the inspection of blood spatter patterns which were produced due to violent crimes [1]. The goal of BPA is to provide answers to questions arising from the scene of a violent crime such as what caused these patterns. Determination of the region of origin of the blood spatter is expected from the BPA community [2], however, current techniques lack a fundamental basis in fluid mechanics [3]. Namely, the method of strings, or the trigonometric method, which has been in use since as early as the 1950s [4] and is implemented in widely distributed software [5–9], neglects physical realities such as gravity and air drag [2]. Understandably, this results in significant well-established errors [10,11], for example, there can be a 50% overestimation of the height of the region of origin [12]. Moreover, the widely used formula for the determination of the impact angle of a blood droplet, $\sin \alpha = W/L$ [13], where W is the width of the stain and L is the length, has major flaws since the values of sine of the impact angle are practically indistinguishable between 75° and

90°. Namely, they vary from 0.97 for 75° and 1 for 90°, and is the reason that standard BPA practice encourages stains with impact angles less than 60° be used for reconstruction [1].

Adding to the difficulty of an accurate reconstruction model of blood spatter patterns is the rheological complexity of blood. Blood is a non-Newtonian, shear thinning [14–16] complex aqueous solution containing various cells and proteins in plasma, and begins to coagulate as soon as it is outside of the human body [17,18]. Moreover, its rheological behavior depends on the hematocrit [14,19], it exhibits viscoelasticity [16,19–21] and possesses a yield stress [22]. This rheological behavior is important in crime scene reconstruction because it can affect the atomization process [23–26], which is diminished in liquids which exhibit viscoelastic properties [26–28]. Resultant droplet sizes are also influenced by these effects [29–34] as well as their final impact on surfaces [31,35,36]. Additionally, blood droplets are spattered at body temperature and often are subject in flight to air at a different temperature, the effects of which have been investigated [37], but never in the context of BPA.

With some of these challenges in mind, several models have been developed to attempt to better recreate crime scenes. Including the effect of drag via a probabilistic approach was proposed in Refs. [38,39]. Further still, in Ref. [40], both gravity and

* Corresponding author.

E-mail address: ayarin@uic.edu (A.L. Yarin).

air drag were accounted for which allowed for the region of origin of the bloodstains to be determined with about four times the accuracy over the method of strings. However, these methods do not explain and consider how blood droplets form due to a gunshot. Rather, they take existing bloodstain patterns and reconstruct blood droplet trajectories without considering the physical causes of droplet formation. This was mitigated in Refs. [41] and [42] by linking the resultant backward flow field of blood from a bullet impact to the Rayleigh–Taylor instability, and then, to the droplet formation and trajectories, determined by gravity, air drag, and droplet-droplet aerodynamic interactions. The Rayleigh–Taylor instability arises when denser blood is accelerating towards lighter air [43], as is the case of blood backward spatter splashing due to a gunshot. Recently, spatter patterns resulting from blood droplets in the direction of bullet motion, i.e. forward spatter, was explored in detail and shown to be fundamentally different from backward spatter [44,45].

In the present work, the experimental investigations of Refs. [41] and [42] were expanded upon and directly compared with their respective predictive models. Moreover, the models are utilized to offer further insight by predicting the locations of the stain area corresponding to a 50% cumulative distribution and the geometric centroid of the stains as a function of distance to impingement. The experiments are described in Section 2, a brief overview of the predictive models is given in Section 3 along with the comparison with the data and further insights, and finally, conclusions are drawn in Section 4.

2. Experimental investigations

The experiments in this paper are a subset of an open source data set of high-resolution (600 DPI) scanned images of blood spatter from a gunshot [46]. There, the experimental conditions are described in detail, and allows the forensic science community to test their models on publicly available data. Backward spattered blood droplets due to a gunshot were created at the Izaak Walton League Park indoor shooting range in Ames, Iowa, USA. While the indoor shooting range provided quiescent air for the experiments, the environmental conditions varied with the time of the year of the specific experiments. Relative humidity was measured between 44% and 76%, with a precision of $\pm 5\%$ and room temperature was between 14.5 and 23.5 °C. The rifle used was a 0.223 cal Rock River Arms, LAR-15 16" barrel M-4, fit with a Yanki YHM Phantom 223 suppressor firing two different types of bullets, one hollow point, and the other full metal jacket. The hollow point bullet was a BEE 0.224 cal with a 0.223 Remington casing, 26.5 grain BLC-2 powder, and Winchester Small Rifle Primer. The full metal jacket bullet was a 5.56 mm caliber Federal Ammunition XM193 with a mass of 55 grain. The velocity of the hollow point bullet was measured with a chronograph as 897 m/s, and the full metal jacket bullet was measured to be 922 m/s.

The bullets were shot at either a closed hollow cavity or polyurethane foam sheet filled with 10–13 mL of swine blood. For the experiments conducted with the soaked foam target, the blood was anticoagulated with ACD and had 41% hematocrit. The temperature of the blood injected into the foam was 35 ± 2 °C. For the experiments where blood was contained in a closed hollow cavity, the blood was used at room temperature and anticoagulated with heparin and had 38–39% hematocrit. In each case, the blood was drawn two days before the experiment was conducted. A schematic of the experimental setup is depicted in Fig. 1.

Having in mind the effect of expanding muzzle gases interacting with blood droplets in flight [47], the experimental setup was designed such that the bullet penetrated through a sheet

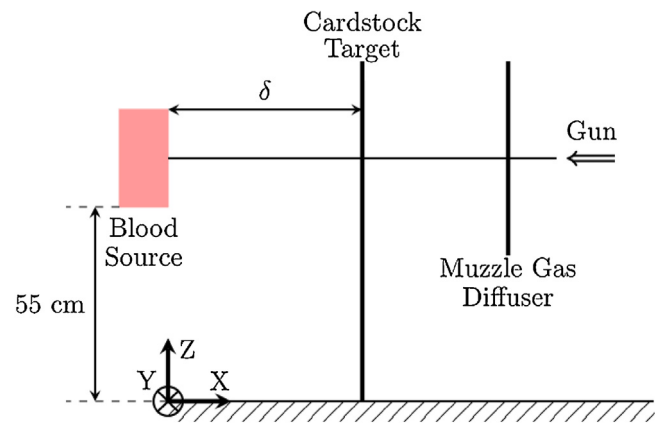


Fig. 1. Schematic of the experimental setup used to generate backward spattered blood droplets impacting on a vertical substrate. Variables are dependent upon which experiment was conducted as specified in Table 1. The coordinate trihedron is located on the floor, with the X-axis being parallel and coplanar (with respect to the Z–X plane) to the path of the bullet which was aimed at the target center.

of cardstock which acted as a diffuser to obstruct the muzzle gases from travelling downstream. The substrate which was impacted by the blood droplets was smooth cardstock.

3. Predictive models

The impact phenomenon of a bullet in which the backward spatter of blood results from is a short-term event. Given a bullet penetration depth of $h \approx 1$ cm, and a bullet impact velocity of $V_0 \approx 300$ m/s, the penetration time is $\tau \approx 33 \mu\text{s}$ which indicates that inertial forces dominate over the viscous ones. The strong, short-term impact of a blunt bullet results in an almost instantaneous pressure field which generates backward flow in the framework of potential impulsive flow hydrodynamics with pressure being the potential [48–50]. For a Newtonian viscous liquid, such an impulsive irrotational potential impact flow sets in when the dimensionless group $\mu u / (Lp) \ll 1$, where μ is the viscosity, u is the fluid velocity (in the flow starting from rest), p is the pressure acting on fluid, and L is the characteristic length scale. On the other hand, penetration of a sharp bullet proceeds under dominant inertial forces, and thus, is potential in the ordinary hydrodynamic sense. The latter case corresponds to the seminal Wagner problem [50,51]. Potential flows are irrotational and remain as such for the entire duration of the aforementioned flows under the conditions of Kelvin's Circulation Theorem [48–50].

Accordingly, the methods developed to predict backward splashed blood flow resulting from sharp [41] and blunt bullets [42] are based on their corresponding incompressible potential flows which satisfy the Laplace equation with appropriate boundary conditions. A diagram of the two cases with their variable definitions is shown in Fig. 2.

For a blunt bullet the initial blood velocity, v , and acceleration, A , at the target surface are, respectively,

$$v = \frac{2}{\pi} V_0 \left[\frac{a}{\sqrt{r^2 - a^2}} - \arcsin\left(\frac{a}{r}\right) \right], \quad (1)$$

$$A = \frac{2V_0^2}{\pi c a} \left[\frac{a}{\sqrt{r^2 - a^2}} - \arcsin\left(\frac{a}{r}\right) \right], \quad (2)$$

where a is the radius of the edge of the blunt bullet, r is the radial coordinate with the origin at the axis of symmetry, and c a dimensionless factor associated with the time scale of the impulsive motion [42].

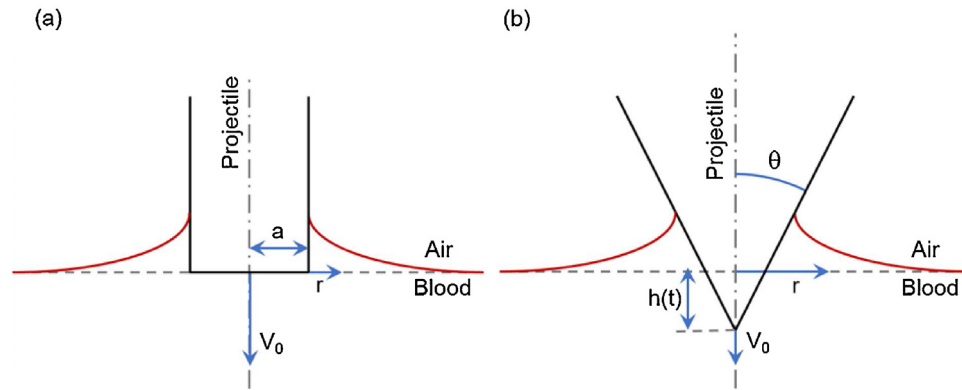


Fig. 2. Mathematical diagrams of the two problems for the reconstruction of trajectories in backward spatter for (a) the blunt bullet, and (b) the sharp bullet.

The factor c is dictated by the time scale of impulsive motion [42] which is a function of the impact velocity of the bullet. However, this factor most likely does not drastically change from bullet to bullet, even though their impact velocities may be drastically different. The reason for this is that the timescale of impact phenomena with a bullet is very short, regardless of the bullet type.

For the initial moments of penetration of a sharp bullet, the initial velocity and acceleration of the blood at the target surface are respectively,

$$v = \frac{\theta^2 V_0 h}{r}, \quad (3)$$

$$A = \frac{\theta^2 V_0^2}{r}, \quad (4)$$

where θ is the semi-angle of the bullet generatrix, and h is the depth of bullet penetration which is a function of the time since impact, t . Note that the depth of bullet penetration h can be predicted as a function of time t , for example, using Eqs. (17) and (18) from Ref. [41].

Eqs. (2) and (4) describe the acceleration of denser blood at the free surface towards lighter air. Such a situation is inherently unstable and results in the Rayleigh–Taylor instability [43]. This instability results in the characteristic droplet sizes, l_* , issued backward from the free surface, which is given by the following expression,

$$l_* = \frac{2\pi}{\sqrt{\rho A/(3\sigma)}} w, \quad (5)$$

where ρ is the density of the blood (1060 kg/m^3 [16]), σ is its surface tension (60.45 mN/m [16]), and w is a dimensionless factor. A possible variation of the density and surface tension with temperature is not included in the models discussed here, because for liquids, surface tension variation in a reasonable temperature interval is not large, and, moreover, surface tension σ enters Eq. (5) as $\sqrt{\sigma}$, which minimizes the effect of temperature even further. The density variation with temperature is practically insignificant.

The Rayleigh–Taylor instability links the flow field of blood in the target splashed backward by a gunshot to the generation of individual droplets, a link which common BPA techniques such as the method of strings, do not contain. This makes the aforementioned models [41,42] physical in nature, i.e. linking the blood spatter pattern to the bullet shape and the gunshot parameters. Note also that in Ref. [42], the spray angle of blood droplets from the target with respect to the axis of the bullet was predicted to be 13° using the hydrodynamic theory of turbulent submerged jets.

The splashed blood droplet trajectories are predicted by models [41,42] using momentum balance equations accounting for the effects of gravity and air drag affected by droplet-droplet aerodynamic interactions (the latter being a collective effect). This collective effect stems from the entrainment of air by the leading droplets, the aerodynamic wake of which diminishes air drag on the subsequent droplets and can even accelerate them, as shown in Ref. [52] and highlighted in Fig. 3. This is similar to a flock of geese flying in V-formation where the leading goose experiences larger air drag than those behind it and thus essentially pulls the others. Eventually, the leading goose will be switched to a position in the back of the formation and this results in a flock which can fly further [53]. The bullet used to create the velocity history plot of Fig. 3 closely resembles a sharp one and as such can help further validate the framework of the models. The range of initial velocities predicted with Eq. (3) is superimposed on Fig. 3 and shows that the calculated values are appropriate. Furthermore, the data used in Fig. 3 allows for an average 2D area to be found from the droplets which experimentally was 0.084 mm^2 , whereas assuming a circular area with the diameter calculated in Eq. (5), the theory predicts an average droplet area of 0.079 mm^2 .

For the simulation of the backward spatter of blood on a vertical wall (cf. Fig. 1), the cardstock target was discretized into 10 even rings spanning the minimum and maximum radial distances from the bullet penetration hole. The median distance of each ring from the center of the hole is R . For the number of stains, the stains in each ring were added together, for the stain area and impact angle, they were averaged in each ring. Comparisons of the predicted and

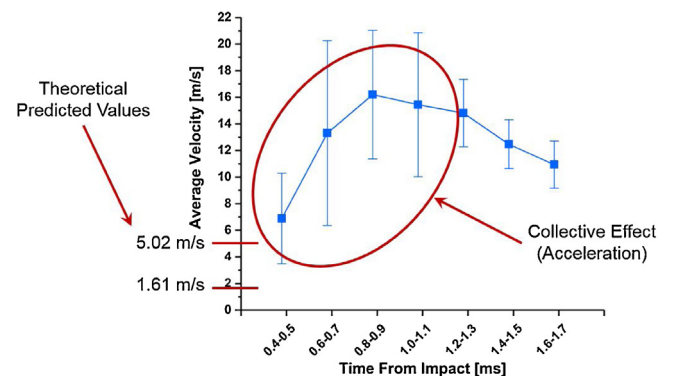


Fig. 3. Average velocity of droplets splashed in backward spatter due to a gunshot as a function of time found from particle image velocimetry of a high-speed video [52]. The error bars represent standard deviation. The velocity is initially increasing because the continued acceleration of flying droplets due to the pulling effect of the aerodynamic wake of the leading blood droplets producing a collective effect. The initial velocities predicted using Eq. (3) are shown.

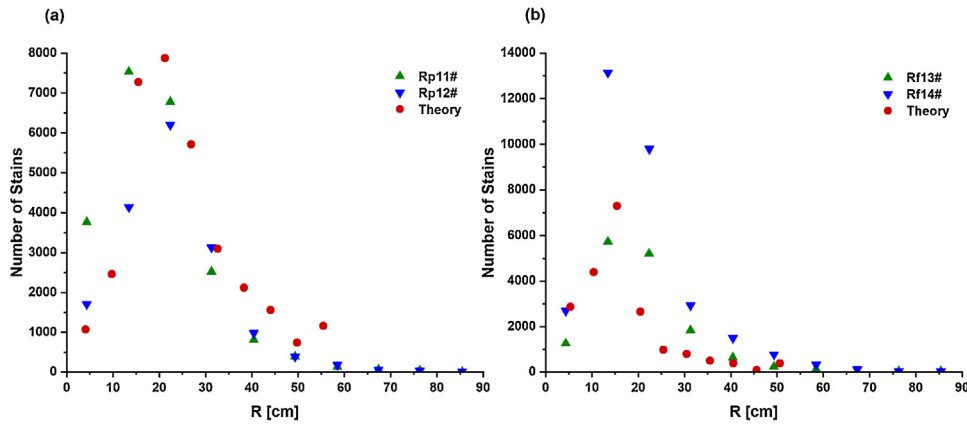


Fig. 4. Number of stains on a vertical wall in the case of (a) a sharp bullet and (b) a blunt bullet. The red circles show the theoretical predictions and the triangles correspond to the experimental trial numbers in Table 1. (For interpretation of the references to colour in this figure legend, the reader is referred to the web version of this article.)

measured number of stains resulting from the sharp and blunt bullets are shown in Fig. 4.

The resultant stain area, S , is a function of the droplet final velocity and size, which is amplified on impact according to the spread factor [29,54,55], as well as the final impact angle, α , reckoned from the vertical as Ref. [13],

$$S = \frac{\pi l_s^2 \xi}{4 \sin \alpha}, \quad (6)$$

where ξ is the droplet spread factor calculated with the Reynolds number of the impacting blood droplet at high shear rates, $\mu_{\text{shear}} = 5 \text{ mPa} \cdot \text{s}$ [16]. Specifically, the original droplet velocity and size are predicted from Eqs. (3) and (5), respectively. After that, the trajectories are calculated as described in Ref. [42], and then, the spreading factor ξ is found from Eq. (29) in Ref. [42].

For the same conditions as in Fig. 4, a comparison of the theoretical predictions with the experimental data for the average

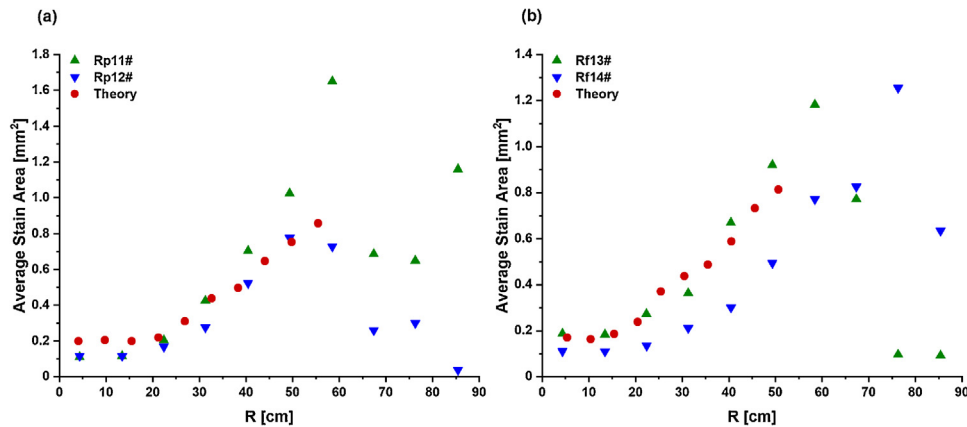


Fig. 5. Average stain area of droplets impacting onto a vertical wall for (a) a sharp bullet and (b) a blunt bullet. Same notations as in Fig. 4.

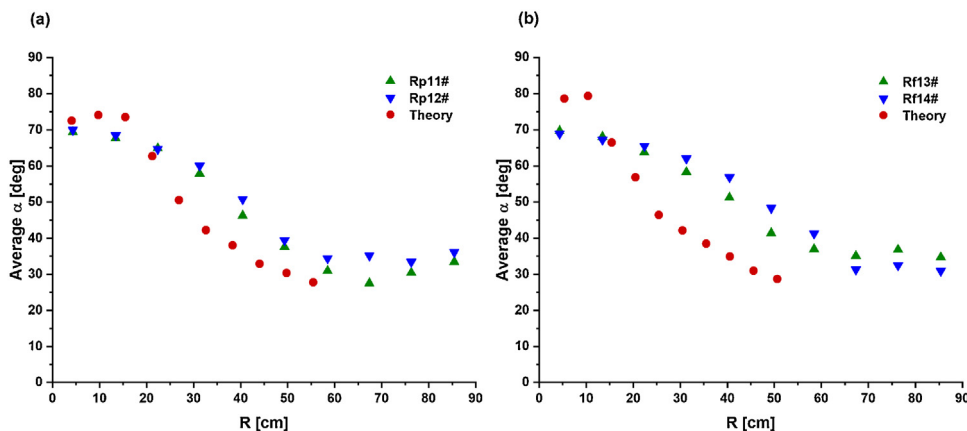


Fig. 6. Average impact angle relative to a vertical wall for (a) a sharp bullet and (b) a blunt bullet. Same notations as in Figs. 3 and 4. A value of $\alpha_{\text{Avg}} = 90^\circ$ corresponds to normal impact.

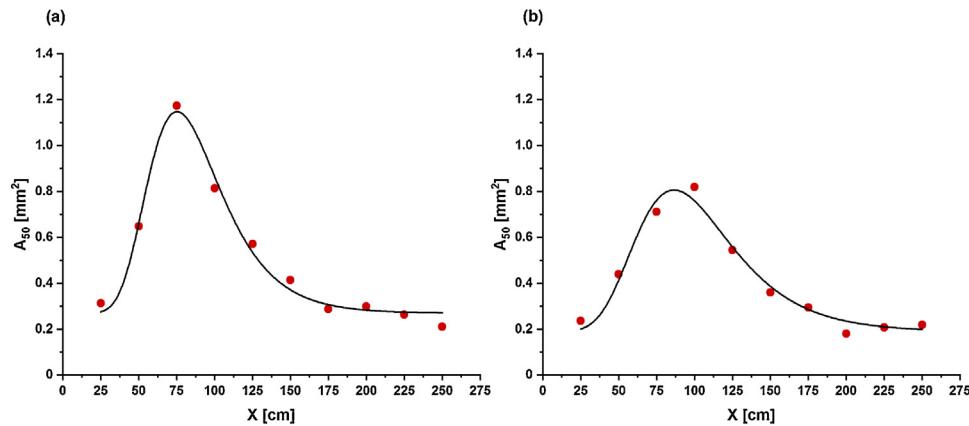


Fig. 7. Area corresponding to 50% of the cumulative distribution of area as a function of the vertical impact substrate distance. Panel (a) is for a sharp bullet and (b) for a blunt bullet. The red circles are the results of the theoretical codes and the black line a best fit function. (For interpretation of the references to colour in this figure legend, the reader is referred to the web version of this article.)

Table 1

Parameters of the experiments of different blood backward spatter situations. The variables are defined in Fig. 1, HP stands for the hollow point bullet, FMJ for the full metal jacket bullet, V_{Blood} for the volume of blood used in the target, and the blood source corresponds to either a soaked polyurethane foam (a) or a hollow cavity (b). For all experiments the bullet impacted the target normally.

Experiment number	Bullet	Substrate	Blood source	δ [cm]	V_{Blood} [mL]
Rp11#	FMJ	Cardstock	(a)	50	13
Rp12#	FMJ	Cardstock	(a)	50	13
Rf13#	HP	Cardstock	(a)	50	13
Rf14#	HP	Cardstock	(a)	50	13
Rp41	FMJ	Cardstock	(b)	10	10
Rp42	FMJ	Cardstock	(b)	30	10
Rp43	FMJ	Cardstock	(b)	30	10
Rp44	FMJ	Cardstock	(b)	30	10
Rp45	FMJ	Cardstock	(b)	60	10
Rp46	FMJ	Cardstock	(b)	60	10
Rp47	FMJ	Cardstock	(b)	60	10
Rp48	FMJ	Cardstock	(b)	120	10
Rp49	FMJ	Cardstock	(b)	120	10
Rp50	FMJ	Cardstock	(b)	120	10
Rp101	FMJ	Cardstock	(b)	90	10

Table 2

Parameters in the best fit correlation of Eq. (7), used for the stain area corresponding to 50% of the cumulative distribution of area. The values within the parenthesis represent standard error and the last row is the coefficient of determination.

	Sharp bullet	Blunt bullet
A_0	0.269 (0.022)	0.190 (0.029)
B	0.877 (0.046)	0.616 (0.042)
C	75.219 (1.408)	86.481 (2.278)
D	24.033 (1.657)	31.643 (3.166)
R^2	0.978	0.959

stain area (it should be emphasized that this is averaged in each ring) is shown in Fig. 5.

The average impact angles predicted and measured under the same conditions as in Figs. 4 and 5 are shown in Fig. 6.

The two predictive models of backward spatter of blood [41,42] can offer further insight to better understand various physical scenarios which BPA experts can use to quantitatively analyze crime scenes. Applying both models with the same parameters fitted to the experiments used in Figs. 4–6 and changing the distance between the blood source and the vertical cardstock target from 25 to 250 cm in steps of 25 cm, allows for cross-sections of the evolution of the blood droplet spray to be seen. The cumulative stained area was plotted as a function of the area of the

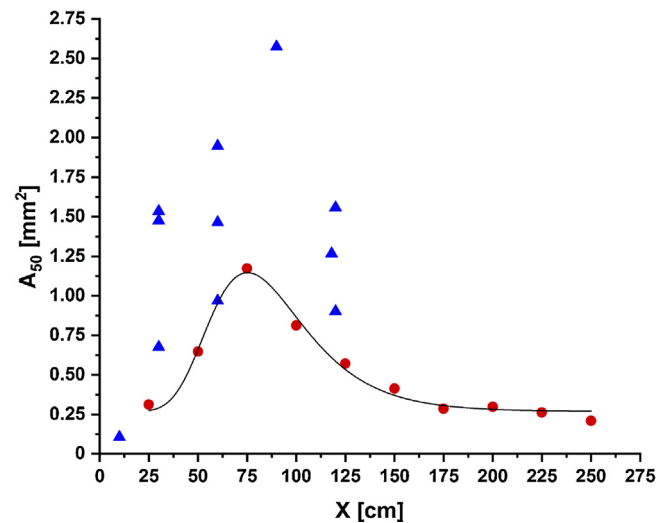


Fig. 8. Comparison between experiments and the numerical simulation of A_{50} for the sharp bullet case. The blue triangles represent experimental trials Rp41–Rp50, and Rp101 in Table 1, and the red circles and line are the results of the numerical simulations shown in Fig. 7(a). (For interpretation of the references to colour in this figure legend, the reader is referred to the web version of this article.)

Table 3

Parameters in the best fit correlation of Eq. (8) used for the centroid locations C_y . The values within the parenthesis represent standard error and the last row is the coefficient of determination.

	Sharp bullet	Blunt bullet
C_0	53.591 (4.319)	48.273 (5.973)
F	184.433 (36.009)	162.898 (22.526)
G	0.028 (0.006)	0.0190 (0.004)
R^2	0.937	0.946

stains in the spatter, a statistical concept that has been found useful to describe beating spatters [56]. Then, the value corresponding to 50% of the cumulative distribution, denoted as A_{50} and plotted as a function of the vertical substrate location, is shown in Fig. 7.

The best fit lines of Fig. 7 are useful for interpolating distance between those at which data points were taken. An appropriate fit was created with the equation,

$$A_{50} = A_0 + (B)e^{-\exp(-\lambda) - \lambda + 1}, \quad (7)$$

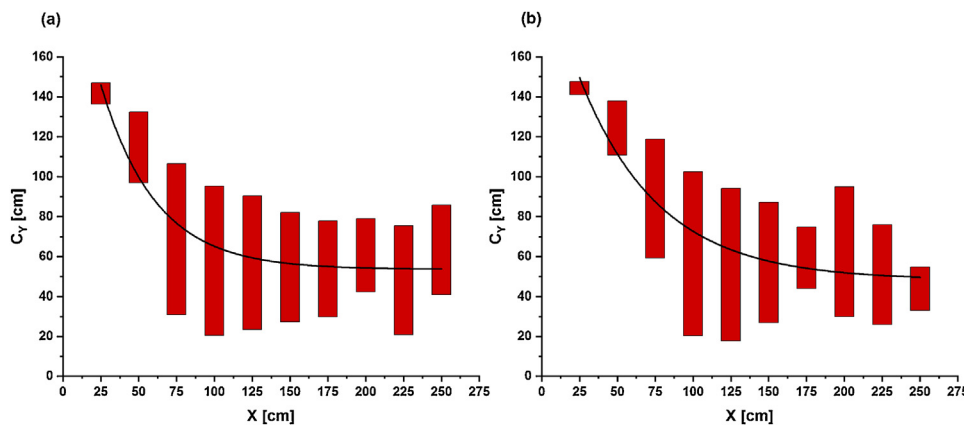


Fig. 9. The geometric centroid bounded by small and large droplets corresponding to A_{50} . Panel (a) is for a sharp bullet and (b) for a blunt bullet. The red bars are the result of the theoretical codes and the black line is the best fit. (For interpretation of the references to colour in this figure legend, the reader is referred to the web version of this article.)

where $\lambda = (Z - C)/D$ and the values of the parameters are listed in Table 2.

It is interesting to note that in Fig. 7, the sharp bullet produces larger droplets and at closer vertical deposition distances than its blunt bullet counterpart. The prediction from the numerical simulations in Fig. 7 that A_{50} reaches a maximum at an intermediate distance between blood source and vertical target spatter was tested against a series of gunshot backspatter experiments from Ref. [46]. As Fig. 8 shows, both experiments and numerical simulations show a comparable maximum for A_{50} at a distance of about 75–90 cm. This agreement between experiments and numerical simulations is a sign that the developed model captures the relevant fluid dynamics. Moreover, it opens a path towards quantitative crime scene reconstruction of the relative position of the blood source and the spatter based on a statistical examination of the stains.

The A_{50} value for each vertical deposition distance acts as a border between the small and large droplets. The geometric centroids, C_Y , of those less than or equal to this value as compared to those larger than A_{50} , can help facilitate a qualitative analysis performed by BPA experts on the distance to the vertical impact substrate by comparing to the quantitative analysis below. Plotting the lowest bounded centroid (from droplets $> A_{50}$) and the highest bounded centroid (from droplets $\leq A_{50}$) as a function of the vertical deposition distance is seen in Fig. 9.

Note that C_Y becomes the same and equal to approximately 60 cm for both bullet types after a certain distance. The best fit lines of Fig. 8 were found based off of the average of the two centroids and a good fit was found with a simple exponential decay function,

$$C_Y = C_0 + Fe^{-CZ}, \quad (8)$$

where the parameters are shown in Table 3.

4. Conclusion

A series of experiments were conducted by the present group and the resultant experimental images with the raw data deposited in Ref. [46]. Four of those sets of experimental data were chosen and compared with the physically based models for sharp [41], and blunt bullets [42]. These models predict that the Rayleigh–Taylor instability is responsible for blood droplet formation in backward spatter and their initial size distribution. The velocity and acceleration distribution in blood in the target are found solving the corresponding fluid mechanical problem, thus allowing for the prediction of the resulting trajectories of the

droplets accounting for gravity, air drag and droplet-droplet aerodynamic interactions. The number of stains, the average stain area, and the average impact angle on the cardstock target predicted by the physical models of Refs. [41,42] were compared with experimental data and revealed reasonably good agreement. Also, the models were used to provide a further insight into the phenomena of backward spattered blood by predicting the locations of the stain area corresponding to a 50% cumulative distribution and the geometric centroid of the spatter pattern. It should be emphasized that the proposed empirical formulae of Eqs. (7) and (8) have not been extensively tested against a variety of gunshot spatter patterns. However, they have originated from the experiments and predictions mentioned in this work which provides an initial step on the path towards quantitative crime scene reconstruction.

Acknowledgements

This work was financially supported by the United States National Institute of Justice (award NIJ 2014-DN-BX-K036 and NIJ 2017-DN-BX-0171). The authors gratefully acknowledge Dr. David P. Baldwin for fruitful discussions on the application of cumulative percent area curves.

References

- [1] T. Bevel, R.M. Gardner, *Bloodstain Pattern Analysis with an Introduction to Crime Scene Reconstruction*, CRC, Boca Raton, 2008.
- [2] S. Weidman, Strengthening Forensic Science in the United States: A Path Forward, Committee on Identifying the Needs of the Forensic Sciences Community, National Research Council, 2009. <http://www.nap.edu/catalog/12589.html>.
- [3] D. Attinger, C. Moore, A. Donaldson, A. Jafari, H.A. Stone, Fluid dynamics topics in bloodstain pattern analysis: comparative review and research opportunities, *Forensic Sci. Int.* 231 (2013) 375–396.
- [4] P.L. Kirk, Affidavit Regarding State of Ohio vs Samuel H. Sheppard, Court of Common Pleas, Criminal Branch, No. 64571, 26 April 1955.
- [5] M.B. Illes, A.L. Carter, P.L. Latusus, A.B. Yamashita, Use of BackTrack™ computer program for bloodstain pattern analysis of stains from downward-moving drops, *J. Can. Soc. Forensic Sci.* 38 (2005) 213–218.
- [6] A.L. Carter, The directional analysis of bloodstain patterns: theory and experimental validation, *J. Can. Forensic Sci.* 34 (2001) 173–189.
- [7] R. Kanable, BackTrack going forward, *Law Enforcement Technol.* 40 (August) (2006) 46–48.
- [8] A.L. Carter, J. Forsythe-Erman, V. Hawkes, A.B. Yamashita, Validation of the BackTrack™ suite of programs for bloodstain pattern analysis, *J. Forensic Identif.* 56 (2006) 242–254.
- [9] A.L. Carter, M. Illes, K. Maloney, A.B. Yamashita, B. Allen, B. Brown, L. Davidson, G. Ellis, J. Gallant, A. Gradkowski, J. Hignell, S. Jory, P.L. Latusus, C.C. Moore, R. Pembroke, A. Richard, R. Spennard, C. Stewart, Further validation of the BackTrack™ computer program for bloodstain pattern analysis: precision and accuracy, *Int. Assoc. Bloodstain Pattern Analysts News* 21 (2005) 15–22.

- [10] W.F. Rowe, Errors in the determination of the point of origin of bloodstains, *Forensic Sci. Int.* 161 (2006) 47–51.
- [11] K.G. de Bruin, R.D. Stoel, J.C.M. Limborgh, Improving the point of origin determination in bloodstain pattern analysis, *J. Forensic Sci.* 56 (2011) 1476.
- [12] N. Behrooz, L. Hulse-Smith, S. Chandra, An evaluation of the underlying mechanisms of bloodstain pattern analysis error, *J. Forensic Sci.* 56 (2011) 1136–1142.
- [13] C. Rizer, *Police Mathematics*, Thomas, Springfield, 1955.
- [14] S. De Gruttola, K. Boomsma, D. Poulikakos, Computational simulation of a non-Newtonian model of the blood separation process, *Artif. Org.* 29 (2005) 949–959.
- [15] S. Charm, G. Kurland, Viscometry of human blood for shear rates of 0–100,000 sec^{-1} , *Nature* 4984 (1965) 617–618.
- [16] A. Kolbasov, P.M. Comiskey, R.P. Sahu, S. Sinha-Ray, A.L. Yarin, B.S. Sikarwar, S. Kim, T.Z. Jubery, D. Attinger, Blood rheology in shear and uniaxial elongation, *Rheol. Acta* 55 (2016) 901–908.
- [17] E.W. Davie, K. Fujikawa, Basic mechanisms in blood coagulation, *Ann. Rev. Biochem.* 44 (1975) 799–829.
- [18] J.J. Hathcock, Flow effects on coagulation and thrombosis, *Arterioscler. Thromb. Vac. Biol.* 26 (2006) 1729–1737.
- [19] S. Chien, R.G. King, R. Skalak, S. Usami, A.L. Copley, Viscoelastic properties of human blood and red cell suspensions, *Biorheology* 12 (1975) 341–346.
- [20] A.L. Copley, R.G. King, S. Chien, S. Usami, R. Skalak, C.R. Huang, Microscopic observations of viscoelasticity of human blood in steady and oscillatory shear, *Biorheology* 12 (1975) 257–263.
- [21] M. Brust, C. Schaefer, R. Doerr, L. Pan, M. Garcia, P.E. Arratia, C. Wagner, Rheology of human blood plasma: viscoelastic versus Newtonian behavior, *Phys. Rev. Lett.* 110 (2013) 078305.
- [22] C. Picart, J.M. Piau, H. Galliard, P. Carpentier, Human blood shear yield stress and its hematocrit dependence, *J. Rheol.* 42 (1998) 1–12.
- [23] S.P. Lin, R.D. Reitz, Drop and spray formation from a liquid jet, *Annu. Rev. Fluid Mech.* 30 (1998) 85–105.
- [24] J. Eggers, E. Villermaux, Physics of liquid jets, *Rep. Prog. Phys.* 71 (2008) 036601.
- [25] A.L. Yarin, *Free Liquid Jets and Films: Hydrodynamics and Rheology*, Longman Scientific & Technical and John Wiley & Sons, New York, 1993.
- [26] C. Clasen, J. Bico, V.M. Entov, G.H. McKinley, 'Gobbling drops': the jetting-dripping transition in flows of polymer solutions, *J. Fluid Mech.* 636 (2009) 5–40.
- [27] D.D. Joseph, J. Belanger, G.S. Beavers, Breakup of a liquid drop suddenly exposed to a high-speed airstream, *Int. J. Multiph. Flow* 25 (1999) 1263–1303.
- [28] F. Mighri, P.J. Carreau, A. Ajji, Influence of elastic properties on drop deformation and breakup in shear flow, *Soc. Rheol.* 42 (1998) 1477–1490.
- [29] A.L. Yarin, Drop impact dynamics: splashing, spreading, receding, bouncing . . . , *Annu. Rev. Fluid Mech.* 38 (2006) 159–192.
- [30] M. Rein, Phenomena of liquid drop impact on solid and liquid surfaces, *Fluid Dyn. Res.* 12 (1993) 61–93.
- [31] V. Bertola, An experimental study of bouncing Leidenfrost drops: comparison between Newtonian and viscoelastic liquids, *Int. J. Heat Mass Transf.* 52 (2009) 1786–1793.
- [32] T. Jiang, J. Ouyang, B. Yang, J. Ren, The SPH method for simulating a viscoelastic drop impact and spreading on an inclined plate, *Comput. Mech.* 45 (2010) 573–583.
- [33] J.J. Cooper-White, R.C. Crooks, D.V. Boger, A drop impact study of worm-like viscoelastic surfactant solutions, *Coll. Surf. A: Physicochem. Eng. Asp.* 210 (2002) 105–123.
- [34] A. Carre, J.C. Gastel, M.E.R. Shanahan, Viscoelastic effects in the spreading of liquids, *Nature* 379 (2002) 432–434.
- [35] D. Caviezel, C. Narayanan, D. Lakehal, Adherence and bouncing of liquid droplets impacting on dry surfaces, *Microfluid. Nanofluid.* 5 (2008) 469–478.
- [36] L. Chen, Z. Li, Bouncing droplets on nonsuperhydrophobic surfaces, *Phys. Rev. E* 82 (2010) 016308.
- [37] D. Poulikakos, J. Waldvogel, Heat transfer and fluid dynamics in the process of spray deposition, *Adv. Heat Transfer* 28 (1996) 1–74.
- [38] B.T. Cecchetto, *Nonlinear Blood Pattern Reconstruction* (MS Thesis), The University of British Columbia, 2010.
- [39] C.R. Varney, F. Gittes, Locating the source of projectile fluid droplets, *Am. J. Phys.* 79 (2011) 838–842.
- [40] N. Laan, K.G. de Bruin, D. Slenker, J. Wilhelm, M. Jermy, D. Bonn, Bloodstain pattern analysis: implementation of a fluid dynamic model for position determination of victims, *Sci. Rep.* 5 (2015) 11461.
- [41] P.M. Comiskey, A.L. Yarin, S. Kim, D. Attinger, Prediction of blood back spatter from a gunshot in bloodstain pattern analysis, *Phys. Rev. Fluids* 1 (2016) 043201.
- [42] P.M. Comiskey, A.L. Yarin, D. Attinger, Hydrodynamics of back spatter by blunt bullet gunshot with a link to bloodstain pattern analysis, *Phys. Rev. Fluids* 2 (2017) 073906.
- [43] S. Chandrasekhar, *Hydrodynamic and Hydromagnetic Stability*, Dover, New York, 1981.
- [44] P.M. Comiskey, A.L. Yarin, D. Attinger, Theoretical and experimental investigation of forward spatter of blood from a gunshot, *Phys. Rev. Fluids* 3 (2018) 063901.
- [45] P.M. Comiskey, A.L. Yarin, D. Attinger, Hydrodynamics of forward blood spattering caused by a bullet of general shape, *Phys. Fluids* (May) (2019) (submitted for publication).
- [46] D. Attinger, Y. Liu, Y. Rao, R. Faflak, K. De Brabanter, P.M. Comiskey, A.L. Yarin, A data set of bloodstain patterns for teaching and research in bloodstain pattern analysis: gunshot backspatters, *Data Brief* 22 (September) (2019) 269–278.
- [47] M.C. Taylor, T.L. Laber, B.P. Epstein, D.S. Zamzow, D.P. Baldwin, The effect of firearm muzzle gases on the backspatter of blood, *Int. J. Leg. Med.* 125 (2011) 617–628.
- [48] G.K. Batchelor, *An Introduction to Fluid Dynamics*, Cambridge University Press, Cambridge, 2002.
- [49] L.G. Loitsyanskii, *Mechanics of Liquids and Gases*, Pergamon, Oxford, 1966.
- [50] A.L. Yarin, I.V. Roisman, C. Tropea, *Collision Phenomena in Liquids and Solids*, Cambridge University Press, Cambridge, 2017.
- [51] H. Wagner, Über Stoß- und Gleitvorgänge an der Oberfläche von Flüssigkeiten, *ZAMM* 12 (1932) 193–215.
- [52] P.M. Comiskey, A.L. Yarin, D. Attinger, High-speed video analysis of forward and backward spatter blood droplets, *Forensic Sci. Int.* 276 (2017) 134–141.
- [53] P.B.S. Lissaman, C.A. Shollenberger, Formation flight of birds, *Science* 168 (1970) 1003–1005.
- [54] B.L. Scheller, D.W. Bousfield, Newtonian drop impact with a solid surface, *AIChE J.* 41 (1995) 1357–1367.
- [55] C. Antonini, A. Amirfazli, M. Marengo, Drop impact and wettability: from hydrophilic to superhydrophobic surfaces, *Phys. Fluids* 24 (2012) 102104.
- [56] D.P. Baldwin, D.S. Zamzow, S.J. Bajic, E. Strawsine, Investigation of impact spatter and the effects of controlled independent variables, *International Association of Bloodstain Pattern Analysts Training Conference* (2013).